Electrochemistry

Received: November 21, 2014
Accepted: February 2, 2015
Published: April 5, 2015

The Electrochemical Society of Japan

http://dx.doi.org/10.5796/electrochemistry.83.262

Article

Electrochemistry, **83(4)**, 262–267 (2015)

Study of Adsorption Behavior and Inhibition Mechanism of Mild Steel in Hydrochloric Acid by a Novel Thiadiazole Derivative

Zhulin CONG,[a,b,c] Weihua LI,[a,b,*] Deping HU,[c,d] Zhenggang LAN,[d] and Baorong HOU[a]

[a] *Institute of Oceanology, Chinese Academy of Sciences, Qingdao 266071, China*
[b] *Cooperative Innovation Center of Engineering Construction and Safety in Shandong Blue Economic Zone, Qingdao 266033, China*
[c] *University of Chinese Academy of Sciences, Beijing 100049, China*
[d] *Key Laboratory of Biobased Materials, Qingdao Institute of Bioenergy and Bioprocess Technoloy, Chinese Academy of Sciences, Qingdao, 266101 Shandong, China*

* *Corresponding author: liweihua@qdio.ac.cn*

ABSTRACT

N′-(4-hydroxy-3-methoxybenzylidene)-2-(5-p-tolyl-1,3,4-thiadiazol-2-ylthio) acetohydrazide (HMTH) was studied as a novel corrosion inhibitor for carbon steel in hydrochloric acid solution by potentiodynamic polarization curves, electrochemical impedance spectroscopy (EIS), chronoamperometry (CA), cyclic voltammetry (CV) techniques and Quantum chemical calculation. The surface morphology of carbon steel in HCl solution in the absence and presence of HMTH was investigated by scanning electron microscopy (SEM). The mechanism of adsorption was determined from Fourier transform infrared spectroscopy (FTIR) and the potential of zero charge (E_{pzc}). HMTH was found to be an effective corrosion inhibitor by forming a stable adsorption layer on carbon steel.

Keywords : Carbon Steel, Acid Solution, Electrochemical Impedance Spectroscopy, PZC

1. Introduction

Carbon steels are used widely in the industry, especially in heat exchanges for their properties such as mechanical strength, good thermal conductivity and low cost. In the production and application process, corrosion products and scale will adsorb on the surface of carbon steel. Hydrochloric acid can quickly dissolve the scale and metal oxides with high efficiency, and allow small permeability of hydrogen. However, hydrochloric acid will cause severe corrosion of carbon steel as well. The use of organic inhibitors is one of the most economical and practical methods of reducing corrosion attack on metals.[1,2] So a considerable amount of effort was devoted to develop novel and efficient corrosion inhibitors.

Most efficient inhibitors are heterocyclic organic compounds consisting of a π-system and/or containing O, N, or S heteroatoms, which can act as the reactive centers playing an important role in the adsorption of inhibitor molecules on the metal surface.[3–8] Thiadiazole is a heterocyclic organic compound, in the molecule of which the nitrogen, sulfur atoms and π-bonds are likely to facilitate the adsorption on the metal surface. And many thiadiazole derivatives have been demonstrated as excellent inhibitors for metals and alloys in acid solutions. HMTH is an organic compound, the molecule of which possesses N, O, S atoms and benzene, thiadiazole rings, which indicates that HMTH can be a good potential inhibitor.

As early as 1996, thiadiazole derivatives were studied as efficient inhibitors for copper corrosion during the process of citric acid treatment.[9] Since then, considerable researches on thiadiazole derivatives as corrosion inhibitors have been conducted for their good corrosion inhibition performances.[9–14] All the researches indicate that thiadiazole derivatives can be good corrosion inhibitors for metals in acid solution. In addition to inhibitive efficiency, the stability and inhibition mechanism of thiadiazole derivatives which are also extremely meaningful research contents have not been investigated in detail until now.

To further study the items above, this research was dedicated to investigate the adsorption and corrosion inhibition mechanism of HMTH on carbon steel in 0.5 M HCl solutions as well as the stability of the surface inhibitor film at anodic and cathodic potentials. Potentiodynamic polarization and EIS technique were used to investigate the inhibition mechanism of HTMH. The stability of inhibitor film was studied by CV and CA techniques at different potentials. Frontier molecular orbital energies were calculated to find the active sites of HTMH which are closely related to the adsorption behavior of inhibitor. FTIR was used to identify if there was adsorption of HMTH on the carbon steel surface. The surface morphology of carbon steel in HCl solutions with and without inhibitor was examined by SEM. The surface charge of carbon steel in 0.5 M HCl was determined by EIS, and a possible inhibition mechanism was proposed.

2. Experimental

2.1 Materials

Tests were performed on carbon steel samples of the following composition (wt %): 0.17% C, 0.46% Mn, 0.26% Si, 0.019% Cu, 0.017% S, 0.0047% P, and the remainder Fe.

N′-(4-hydroxy-3-methoxybenzylidene)-2-(5-p-tolyl-1,3,4-thiadiazol-2-ylthio)acetohydrazide (HMTH) was synthesized following Xue Bai.[15] The chemical structure is given in Fig. 1 and confirmed by NMR spectrum and FT-IR spectroscopic method. ^{1}H NMR (500 MHZ, $CDCl_3$), δ: 2.40 (s,3H,CH3), 3.84 (s,3H,OCH3), 4.06 (s,2H,-SCH2), 6.91–7.76 (m,7H,ArH), 8.15 (s, 1H, CH=N), 8.49

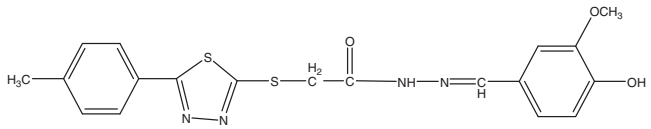

Figure 1. Chemical structure of N′-(4-hydroxy-3-methoxybenzylidene)-2-(5-p-tolyl-1,3,4-thiadiazol-2-ylthio) acetohydrazide (HMTH).

(s,1H,NH), 9.53 (s,1H,OH). IR (KBr):3513, 1613, 1509, 1453, 1277, 1177, 1072, 767 cm^{-1}.

The aggressive solution of 0.5 M HCl was prepared by dilution of a concentrated HCl solution (37%) with distilled water.

2.2 Electrochemical procedure

Electrochemical experiments were carried out in the conventional three electrodes cell with a platinum counter electrode and a saturated calomel electrode (SCE) coupled to a fine Luggin capillary as reference electrode. All working electrodes were made of carbon steel cubic which sealed with epoxy resin to leave only one surface of steel to contact with solutions.[16–19] The surface area of working electrodes was 1.0 × 1.0 cm. All electrodes were abraded with emery paper (grade 600-800-1200), rinsed with distilled water, degreased with acetone, and dried with a cold stream eventually. Before electrochemical measurements, the electrodes were immersed in acid solutions for one hour at open circuit to attain a stable state. All electrochemical measurements were carried out using PARSTAT 2273 electrochemical system.

The potential of potentiodynamic polarization curves was started from a potential of −250 mV to +250 mV versus OCP at a sweep rate of 0.5 mV s^{-1}. Electrochemical impedance spectroscopy (EIS) was carried out at OCP in the frequency range of 10 mHz to 100 kHz. CA experiments were obtained by applying constant potential at ±100 mv vs. corrosion potential which was obtained from potentiodynamic polarization curves for 6000 s. CV measurements were carried out with a scan rate of 10 mV^{-1} by applying 10 segments as described in the literature.[20] In order to discuss the inhibition mechanism, the surface charge of the metal in 0.5 M HCl solution in the presence of HMTH after 1 h was determined by EIS experiments at various potentials.

2.3 Theoretical calculation

The geometry of HMTH molecule was optimized at the ab initio B3LYP level, using 6-31G* basis set with Gaussian09[21] program. And relevant quantum chemical parameters were obtained from this optimized structure.

2.4 FTIR and SEM characterization

FTIR spectra was recorded in a Thermo Scientific Nicolet iS10 FT-IR spectrophotometer. One specimen for FTIR characterization was the HMTH powder. The other was the adsorption layer formed on carbon steel surface after immersion for 1 h in 0.5 M HCl solution containing HMTH. The morphology of the metal surface was studied by scanning electron microscope model SEM Jeol JSM-6700F. Prior to morphology experiments, all specimens were polished as mentioned in electrochemical experiments. SEM micrographs were obtained from metal surface exposed to 0.5 M HCl solution for 3 h in absence and presence of inhibitor.

3. Results and Discussion

3.1 Potentiodynamic polarization curves

Potentiodynamic polarization curves for carbon steel in 0.5 M HCl solutions without and with various concentrations of HMTH are shown in Fig. 2. The values of related electrochemical parameters including corrosion potential (E_{corr}), corrosion current density (i_{corr}), cathodic tafel slope (b_c), anodic tafel slope (b_a) and inhibition efficiency (η%) were calculated from the corresponding polarization curves and are given in Table 1. In this technique, the η% was calculated using the following equation:

$$\eta\% = \left(\frac{i_{corr} - i'_{corr}}{i_{corr}}\right) \times 100 \qquad (1)$$

Where i_{corr} and i'_{corr} represent corrosion current densities in the absence and presence of inhibitor, respectively.

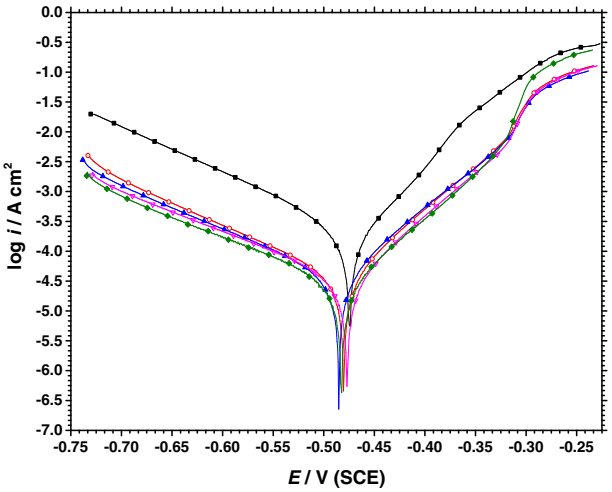

Figure 2. (Color online) Potentiodynamic polarization curves of carbon steel in 0.5 M HCl solution in the absence (■) and presence of 5(○), 10(▲), 15(▽), 20(◆) mg L^{-1} HMTH (immersion time is 1 h).

Table 1. Potentiodynamic polarization parameters for carbon steel in 0.5 M HCl solutions in the absence and presence of different concentrations of HMTH.

C_{ih} (mg L^{-1})	E_{corr} (mV) (SCE)	i_{corr} (μA cm^{-2})	$-b_c$ (mV dec^{-1})	b_a (mV dec^{-1})	η (%)
blank	−475	655	135	74	—
5	−480	34	130	66	94.8
10	−482	32	146	74	95.1
15	−482	30	149	71	95.4
20	−483	26	153	67	96.0

It is apparent that both anodic and cathodic curves shift to lower current densities for the sake of addition of HMTH. In other words, both cathodic hydrogen evolution and anodic metal dissolution reaction of carbon steel are drastically inhibited by HMTH.[22]

From Table 1, it is apparent that i_{corr} decreases considerably with the addition of HMTH. The maximum of η% is 96.0% with 20 mg L^{-1} HMTH. However, η% can reach 94.8% when the concentration of HMTH is only 5 mg L^{-1}, so the trend of η% increasing with the increase of HMTH is not too significant. Generally, if the displacement in E_{corr} is > 85 mV with respect to E_{corr} in uninhibited solution, the inhibitor can be seen as a cathodic or anodic type inhibitor.[23–29] In our study, the maximum displacement in E_{corr} is −8 mV, which demonstrates that HMTH is a mixed-type inhibitor as most other organic inhibitors in the literature.[30–32] b_a and b_c both change little, which indicates that the corrosion mechanism does not change in the presence of HMTH[33] and the inhibition of HMTH works by way of geometric blocking effect.[34] However, it is noteworthy that i_{corr} increases rapidly from −0.320 to −0.280 V (SCE), which can be defined as anodic desorption behavior.[35] This phenomenon mentioned above is mainly referring to desorption of inhibitors from carbon steel surface at high anodic potentials.

3.2 Electrochemical impedance spectroscopy (EIS)

Figure 3 illustrates the Nyquist plots of carbon steel in 0.5 M HCl solutions in the absence and presence of HMTH with different concentrations. The plots of carbon steel with HMTH all show a depressed semi-circular shape at high frequency, which indicates that the corrosion of steel is mainly controlled by a charge transfer process.[36] On the other hand, the small inductive loop of the plot at low frequency in presence of HMTH may be attributed to the

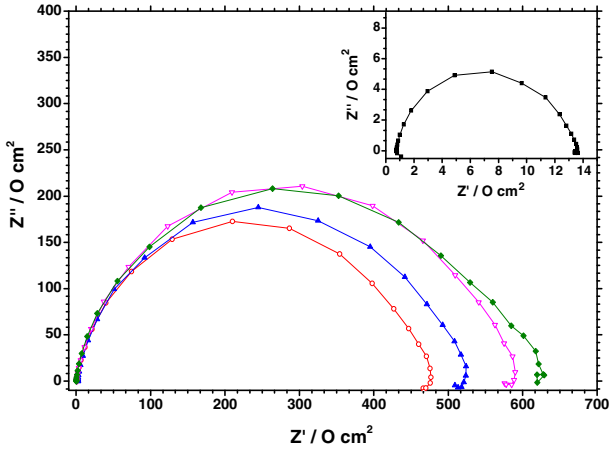

Figure 3. (Color online) Nyquist plots of carbon steel in 0.5 M HCl solution in the absence (■) and presence of 5(○), 10(▲), 15(▽), 20(◆) mg L^{-1} HMTH.

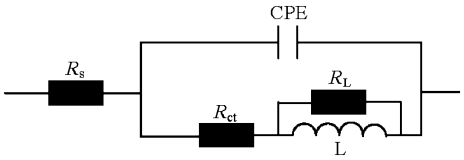

Figure 4. Equivalent circuit used to fit the EIS data.

relaxation process of adsorbed inhibitors on the electrode and/or re-dissolution of the passivated surface.[22] The depression of these capacitive loops is a characteristic of solid electrodes and is often ascribed to dispersion effect, which can be due to the roughness and inhomogeneity on the surface during corrosion.[33] The shape of the Nyquist doesn't change before and after the addition of HMTH, which demonstrates that the corrosion mechanism of carbon steel remains the same.[37] Yet, the diameter of the capacitive loops in the presence of HMTH is quite bigger than that in the absence of HMTH and increases with the inhibitor concentration, which can be ascribed to the forming of the protective layer on the carbon steel surface.

All capacitive loops of EIS spectra were analyzed using the equivalent circuit in Fig. 4. The R_s represents solution resistance and R_{ct} represents charge transfer resistance. L represents inductive and R_L represents inductive resistance. The constant phase element, CPE, is composed of a component of C_{dl} and a coefficient a. The parameter a, is the one mentioned previously, which represents the inhomogeneity of the solid surface. The capacitive of CPE can be expressed by the following expression:

$$C_{dl} = C_{CPE} \times (2\pi f_{max})^{a-1} \quad (2)$$

Where f_{max} represents the frequency at which imaginary value reaches a maximum on the nyquist plot. The parameters of R_{ct}, C_{dl}, and η(%) are presented in Table 2. η% was calculated on the basis of the following equation:

$$\eta\% = \frac{R'_{ct} - R_{ct}}{R'_{ct}} \times 100 \quad (3)$$

It is apparent that the value of R_{ct} increases as the HMTH concentration increases, which indicates that the charge transfer process encounters bigger obstacles due to the adsorption of HMTH. The capacitance decreases considerably with the addition of HMTH, which can be interpreted by the following equation:[34]

$$C_{dl} = \frac{\varepsilon^0 \varepsilon}{d} A \quad (4)$$

Table 2. EIS parameters for carbon steel in 0.5 M HCl solutions in the absence and presence of HMTH.

C_{inh} (mg L^{-1})	CPE (10^6/S^n Ω^{-1} cm^{-2})	n	R_{ct} (Ω cm^2)	η (%)
blank	240	0.93	12.47	—
5	40.7	0.90	304.2	95.9
10	41.8	0.88	389.7	96.8
15	30.4	0.89	566.8	97.8
20	25.6	0.92	581.6	97.9

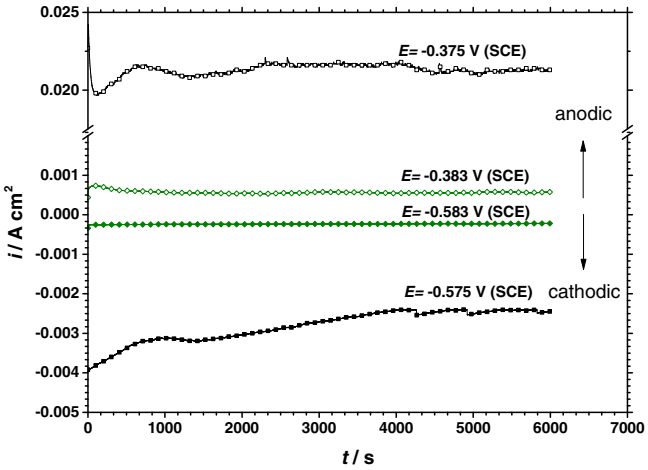

Figure 5. (Color online) CA plots of carbon steel immersing in 0.5 M HCl solution in the absence (□ at anodic potential ■ at cathodic potential) and presence of 20 mg L^{-1} HMTH (◇ at anodic potential ◆ at cathodic potential) for 6000 s.

Where ε^0 is the permittivity of air, ε is the local dielectric constant, d is the thickness of the film and A is the surface area of electrode.

When HMTH was added to the HCl solutions, the big organic inhibitor molecules would replace the small water molecules that absorbed on the steel surface previously. And then this replacement will increase the thickness and decrease the local dielectric constant of the electrical double layer, because organic molecules are bigger in size and with lower conductivity compared to water molecules.[2] The maximum of η% reaches 97.9% in presence of 20 mg/L HMTH, and the growth trend of η% with the increase of HMTH concentration is not significant, which is consistent with the results of potentiodynamic polarization method. This phenomenon can be ascribed to the limitation of the coverage of HMTH on the surface of electrode.

3.3 Stability test

The stability of HMTH inhibitor film was investigated by CA and CV at anodic and cathodic potentials that determined from potentiodynamic polarization curves previously. The CA plots of carbon steel immersing in 0.5 M HCl solutions for 6000 sis presented in Fig. 5.

From Fig. 5 and Fig. 6, it is obvious that the addition of HMTH considerably reduces the corrosion current density of carbon steel in 0.5 M HCl. In Fig. 5, the current densities of carbon steel in 0.5 M HCl with the presence of HMTH at both cathodic and anodic potentials are less than 1 mA cm^2. And the current density in the presence of HMTH changed little in contrast to those in the absence of HMTH. All described above confirms that the HMTH film is quite stable and can protect carbon steel against the attack of acid effectively. Anodic and cathodic CV and CV-time plots are shown in Fig. 6. From CV plots, the curve does not change with the increase

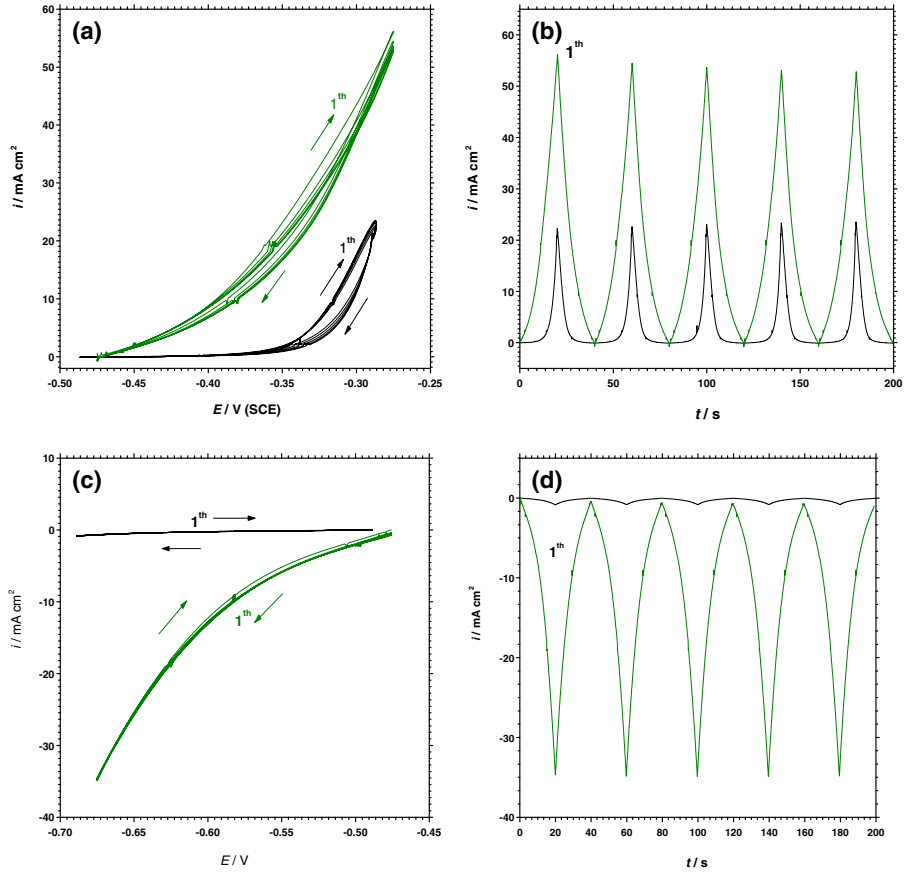

Figure 6. (Color online) Anodic and Cathodic CV (a and c) and CV-time (b and d) plots of carbon steel in 0.5 M HCl solution in the absence (the blank line) and presence (the green line) of 20 mg L^{-1} HMTH.

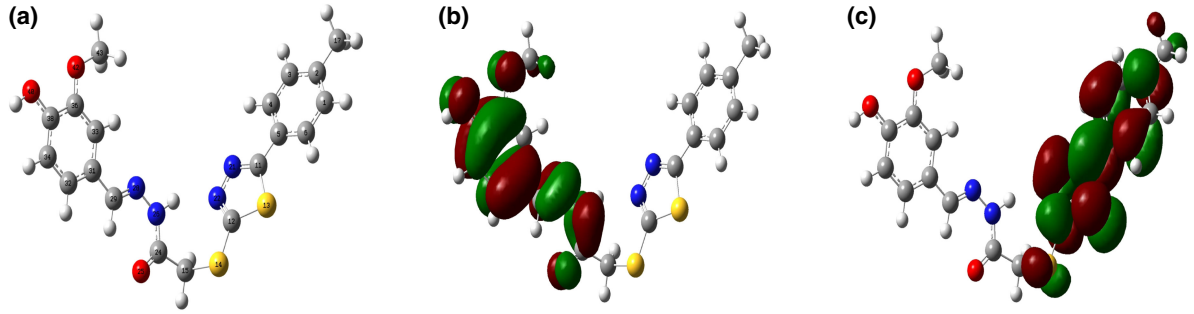

Figure 7. (Color online) Optimized geometry structure (a) and density distribution of HOMO (b) and LUMO (c) of HMTH molecule.

of cycle times in both shape and size, which indicates that there is no desorption of HMTH from the carbon steel surface during the scanning process. The CV-time plots with HMTH also support the conclusion above, which is almost invariable from the first to the last cycle.

3.4 Theoretical calculations

The above experimental results have shown the inhibition efficiency of HMTH, which can resist the attack of acid solution by forming an inhibitor film on the metal surface. Theoretical calculations were applied to investigate the interaction between inhibitor molecules and carbon steel. The optimized geometry structure and density distribution of frontier molecular orbitals (HOMO and LUMO) of HMTH molecule are shown in Fig. 7. The E_{HOMO} value is associated with the ability of the inhibitor molecule to donate electrons to the metal surface, therefore, higher E_{HOMO} values indicate easier donation of electrons from the corrosion inhibitor to the empty metal d orbitals. On the contrary, lower values of this property means that the inhibitor accommodates additional negative charge from the metal surface more easily. The gap energy (ΔE) is usually of great importance in describing the static molecular reactivity. The molecules with lower energy band gap exhibit higher inhibition efficiencies because low energy gap implies it will be easier to remove an electron from the HOMO orbital to LUMO one and the reactivity of the molecules will increase as a result, which facilitates adsorption and enhances the efficiency of inhibitors.[38–43] The energies of the HOMO and LUMO of the molecule and energy gap ($\Delta E = E_{LUMO} - E_{HOMO}$) were found to be −5.247 eV, −1.861 eV and 3.386 eV, respectively. It is noteworthy that the energy gap is quite low and even lower than most of the efficient inhibitors published before, which means that HMTH exhibits higher inhibition efficiency.[44–49] From Fig. 7, the HMTH molecule is composed of two parts which are almost mutually perpendicular. It can be observed that the HOMO is mainly distributed in the benzene ring on the left, as well as the nitrogen atoms (26, 28) and one oxygen atom (25, 40, 42). It can be induced

that the HOMO will share π electrons with iron atoms and the unshared pair of electrons from the N and O atoms can also donated to the vacant d orbitals of iron atoms.

3.5 Fourier transform infrared spectroscopy (FTIR)

The FTIR spectroscopies of pure HMTH and adsorption layer formed on the carbon steel surface after immersion in 0.5 M HCl containing HMTH are shown in Fig. 8. In the spectrum of HMTH, the characteristic peaks at 3513, 2725, 1613 cm^{-1} are ascribed to O-H, C-H and C=O stretching vibration, respectively. The peaks at 1509 and 1453 $cm^{-1}$are assigned to the framework vibration of benzene rings. The peaks at 1613, 1509, 1453 cm^{-1} all appear in the spectra of adsorption layer on the carbon steel, which indicates that HMTH was adsorbed on the carbon steel surface. The O-H stretching vibration at 3513 cm^{-1} shifting to 3727 cm^{-1} is due to the association of phenolic hydroxyl in aqueous solution. And the disappearance of the peak at 2725 may because the peak at 3727 cm^{-1} is too broad and conceals the peak at 2725 cm^{-1}. The bands at 3727 and 470 cm^{-1} which do not appear in the spectra of HMTH arise from Fe-O bending and Fe-N stretching vibration respectively.[50,51] Comparing the spectra b with a, it is obvious that HMTH is absorbed on the carbon steel surface, and O, N atoms may act as active centers for carbon steel, which is consistent with the results of theoretical calculations.

3.6 Scanning electron microscopy (SEM)

The surfaces of carbon steel specimens after exposing them to 0.5 M HCl solution in the absence and presence of 20 mg HMTH for 2 h were examined by SEM. The SEM images of the mild steel surface are shown in Fig. 9. As it is seen from Fig. 9a, the steel surface is strongly damaged. However, no pits or cracks except polishing lines were observed on the surface of the specimen in HCl solution within HTMH (Fig. 9b). It is obvious that the inhibitor molecules are adsorbed on the carbon steel surface and form a protective film.

3.7 The potential of zero charge (PZC) and the inhibition mechanism

The adsorption of inhibitors mainly depends on surface charge of metals and chemical structure of inhibitor molecules, nature of solution, etc.[52] In order to determine the surface charge state of carbon steel in 0.5 M HCl in the absence and presence of HMTH, EIS experiments were carried out at various potentials (Fig. 10). PZC was obtained according to articles published before.[53] The Antropov's rational corrosion potential (E_r) can be calculated by the following equation:[37]

$$E_r = E_{ocp} - E_{pzc} \quad (5)$$

The E_r is +0.02 V and +0.04 V in 0.5 M HCl in the absence and presence of HMTH respectively, which indicates that carbon steel is positively charged in both solutions. However, the E_{pzc} of carbon steel in presence of HMTH is more negative. In HCl solution, the HMTH molecules may exist in protonated form in equilibrium, which is consistent with the points of Sudhish,[54,55] Pongsak,[56] Demet,[57] Moretti,[58] who presented that organic inhibitors can turn to -onium ions in acid solutions and then adsorb on the negatively charged metals by electrostatic forces. In addition, Haoqing Wu has presented that the E_{pzc} of metals can be more positive when cations absorb on the surface of metal.[59] From the E_{pzc} results, the protonated HMTH molecules may not adsorb on the metal surface directly. The possible adsorption mechanism of HMTH is proposed as follows: (1) Chloride ions will adsorb on metal surface first by

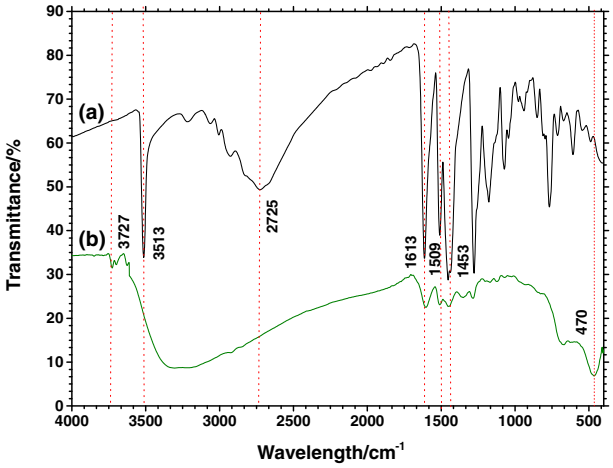

Figure 8. (Color online) FTIR spectra of pure HMTH (a) and adsorption layer (b) formed on the carbon steel surface after immersion in 0.5 M HCl containing HMTH for 3 h.

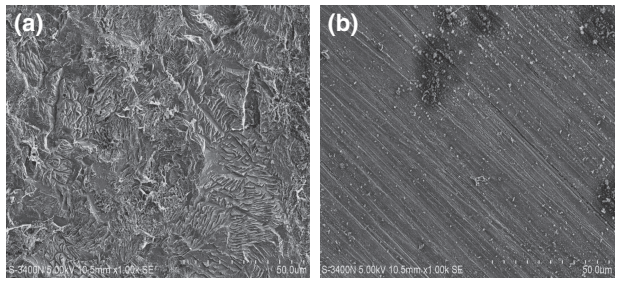

Figure 9. SEM images of the carbon steel surface after exposed to 0.5 M HCl solution for 2 h in the absence (a) and presence of 20 mg HMTH (b).

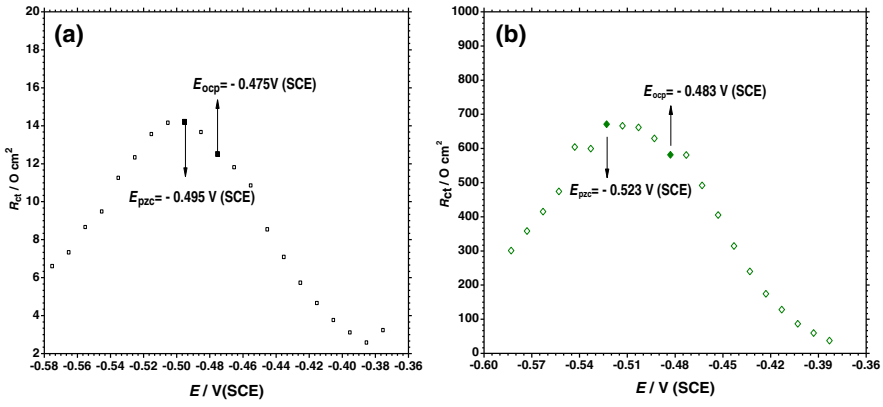

Figure 10. (Color online) R_{ct} plots of carbon steel in 0.5 M HCl solutions in the absence (a) and presence (b) of 20 mg L^{-1} HMTH.

electrostatic forces, which play a role as connecting bridge between the positively charged metal surface and the protonated inhibitor molecules. Then the protonated HTMH molecules adsorb as a result of electrostatic forces. (2) In addition to physical adsorption, the adsorption of HMTH also includes chemical ones which can be ascribed to the donor acceptor interactions between free electron pairs of N, S, O atoms and π electrons of multiple bonds and vacant d orbitals of iron.

As a consequence of all the above interactions, the HTMH molecules adsorb on the surface of carbon steel and form a stable film, which as a protective barrier against the attack of acid solution.

4. Conclusions

(1) HMTH acts as a good inhibitor for the corrosion of carbon steel in 0.5 M HCl solution. The maximum value of $\eta(\%)$ can reach 97.9% with 20 mg L^{-1} HMTH.
(2) HMTH acts as a mixed-type inhibitor in 0.5 M HCl solution. In EIS spectra, the presence of HMTH reduces the values of C_{dl} and enhances R_{ct} values.
(3) The film of HMTH on carbon steel is quite stable at both anodic and cathodic potentials. The current density decreases considerable in the presence of HMTH in HCl solution.
(4) Theoretical calculation results and FTIR spectroscopies revealed that the HOMO mainly distributed in benzene ring and heteroatoms. And the low energy gap suggests HMTH exhibits good inhibition ability.
(5) The PZC methods indicated the carbon steel surface was positive charged in HCl solutions. The difference between the E_{pzc} of carbon steel in absence and presence of HMTH reveal that Chloride ions absorbed on metal surface first, and then HMTH molecules absorbed by electrostatic attraction.

Acknowledgments

The authors gratefully acknowledge the support of National Nature Science Foundation of China (51179182 and 51309212), Outstanding Youth Foundation of Shandong Province (JQ201217) and Qingdao City Guidance Project of Industry-University-Research Collaboration (12-1-4-8-(1)-jch), Science and Technology Projects of Nantong City (BK2013015), Open Research Fund for Key Laboratory of Water Science and Engineering in Ministry of Water Resource (Yk914007). The authors thank the National Supercomputing Center in Shenzhen and the supercomputational center of CAS-QIBEBT for providing computational resources.

References

1. W. H. Li, Q. He, S. T. Zhang, C. L. Pei, and B. R. Hou, *J. Appl. Electrochem.*, **38**, 289 (2008).
2. X. H. Li, S. D. Deng, and H. Fu, *Corros. Sci.*, **62**, 163 (2012).
3. A. Kokalj, S. Peljhan, M. Finsgar, and I. Milosev, *J. Am. Chem. Soc.*, **132**, 16657 (2010).
4. S. Pournazari, M. H. Moayed, and M. Rahimizadeh, *Corros. Sci.*, **71**, 20 (2013).
5. L. Fragoza-Mar, O. Olivares-Xometl, M. A. Domínguez-Aguilar, E. A. Flores, P. Arellanes-Lozada, and F. Jiménez-Cruz, *Corros. Sci.*, **61**, 171 (2012).
6. S. Deng, X. Li, and H. Fu, *Corros. Sci.*, **53**, 822 (2011).
7. A. K. Singh and M. A. Quraishi, *Corros. Sci.*, **52**, 1373 (2010).
8. M. Outirite, M. Lagrenée, M. Lebrini, M. Traisnel, C. Jama, H. Vezin, and F. Bentiss, *Electrochim. Acta*, **55**, 1670 (2010).
9. E. Otero and J. M. Bastidas, *Werkst. Korros.-Mater. Corros.*, **47**, 133 (1996).
10. F. Bentiss, M. Lebrini, M. Lagrenee, M. Traisnel, A. Elfarouk, and H. Vezin, *Electrochim. Acta*, **52**, 6865 (2007).
11. F. Bentiss, M. Traisnel, and M. Lagrenee, *J. Appl. Electrochem.*, **31**, 41 (2001).
12. M. Lebrini, F. Bentiss, H. Vezin, and M. Lagrenee, *Corros. Sci.*, **48**, 1279 (2006).
13. M. Lebrini, M. Lagrenée, H. Vezin, L. Gengembre, and F. Bentiss, *Corros. Sci.*, **47**, 485 (2005).
14. E. M. Sherif and S. M. Park, *Electrochim. Acta*, **51**, 6556 (2006).
15. X. Bai, The Synthesis of N-heterocyclic compounds and study on their inhibitory behavior (2012).
16. S. W. Xia, M. Qiu, L. M. Yu, F. G. Liu, and H. Z. Zhao, *Corros. Sci.*, **50**, 2021 (2008).
17. F. G. Liu, M. Du, J. Zhang, and M. Qiu, *Corros. Sci.*, **51**, 102 (2009).
18. B. Wang, M. Du, J. Zhang, and C. J. Gao, *Corros. Sci.*, **53**, 353 (2011).
19. J. Zhang, X. L. Gong, H. H. Yu, and M. Du, *Corros. Sci.*, **53**, 3324 (2011).
20. R. Solmaz, *Corros. Sci.*, **81**, 75 (2014).
21. M. J. Frisch, G. W. Trucks, H. B. Schlegel, G. E. Scuseria, M. A. Robb, J. R. Cheeseman, G. Scalmani, V. Barone, B. Mennucci, G. A. Petersson, H. Nakatsuji, M. Caricato, X. Li, H. P. Hratchian, A. F. Izmaylov, J. Bloino, G. Zheng, J. L. Sonnenberg, M. Hada, M. Ehara, K. Toyota, R. Fukuda, J. Hasegawa, M. Ishida, T. Nakajima, Y. Honda, O. Kitao, H. Nakai, T. Vreven, J. A. Montgomery, Jr., J. E. Peralta, F. Ogliaro, M. Bearpark, J. J. Heyd, E. Brothers, K. N. Kudin, V. N. Staroverov, R. Kobayashi, J. Normand, K. Raghavachari, A. Rendell, J. C. Burant, S. S. Iyengar, J. Tomasi, M. Cossi, N. Rega, J. M. Millam, M. Klene, J. E. Knox, J. B. Cross, V. Bakken, C. Adamo, J. Jaramillo, R. Gomperts, R. E. Stratmann, O. Yazyev, A. J. Austin, R. Cammi, C. Pomelli, J. W. Ochterski, R. L. Martin, K. Morokuma, V. G. Zakrzewski, G. A. Voth, P. Salvador, J. J. Dannenberg, S. Dapprich, A. D. Daniels, Ö. Farkas, J. B. Foresman, J. V. Ortiz, J. Cioslowski, and D. J. Fox, Gaussian 09, Gaussian, Inc., Wallingford, CT (2009).
22. X. H. Li, S. D. Deng, and H. Fu, *Corros. Sci.*, **53**, 302 (2011).
23. M. A. Hegazy, A. M. Hasan, M. M. Emara, M. F. Bakr, and A. H. Youssef, *Corros. Sci.*, **65**, 67 (2012).
24. L. J. Li, X. P. Zhang, J. L. Lei, J. X. He, S. T. Zhang, and F. S. Pan, *Corros. Sci.*, **63**, 82 (2012).
25. X. H. Li and S. D. Deng, *Corros. Sci.*, **65**, 299 (2012).
26. A. A. Nazeer, N. K. Allam, A. S. Fouda, and E. A. Ashour, *Mater. Chem. Phys.*, **136**, 1 (2012).
27. N. A. Negm, E. A. Badr, I. A. Aiad, M. F. Zaki, and M. M. Said, *Corros. Sci.*, **65**, 77 (2012).
28. N. A. Negm, N. G. Kandile, E. A. Badr, and M. A. Mohammed, *Corros. Sci.*, **65**, 94 (2012).
29. H. Zarrok, A. Zarrouk, B. Hammouti, R. Salghi, C. Jama, and F. Bentiss, *Corros. Sci.*, **64**, 243 (2012).
30. F. Zhang, Y. Tang, Z. Cao, W. Jing, Z. Wu, and Y. Chen, *Corros. Sci.*, **61**, 1 (2012).
31. R. Yıldız, *Corros. Sci.*, **90**, 544 (2015).
32. H. Hamani, T. Douadi, M. Al-Noaimi, S. Issaadi, D. Daoud, and S. Chafaa, *Corros. Sci.*, **88**, 234 (2014).
33. V. V. Torres, V. A. Rayol, M. Magalhaes, G. M. Viana, L. C. S. Aguiar, S. P. Machado, H. Orofino, and E. D'Elia, *Corros. Sci.*, **79**, 108 (2014).
34. X. H. Li, S. D. Deng, and H. Fu, *Corros. Sci.*, **53**, 664 (2011).
35. B. Qiana, J. Wang, M. Zheng, and B. R. Hou, *Corros. Sci.*, **75**, 184 (2013).
36. M. Behpour, S. M. Ghoreishi, N. Mohammadi, N. Soltani, and M. Salavati-Niasari, *Corros. Sci.*, **52**, 4046 (2010).
37. T. Ghailane, R. A. Balkhmima, R. Ghailane, A. Souizi, R. Touir, M. E. Touhami, K. Marakchi, and N. Komiha, *Corros. Sci.*, **76**, 317 (2013).
38. D. Ben Hmamou, R. Salghi, A. Zarrouk, M. R. Aouad, O. Benali, H. Zarrok, M. Messali, B. Hammouti, M. M. Kabanda, M. Bouachrine, and E. E. Ebenso, *Ind. Eng. Chem. Res.*, **52**, 14315 (2013).
39. M. Elbakri, R. Touir, M. E. Touhami, A. Zarrouk, Y. Aouine, M. Sfaira, M. Bouachrine, A. Alami, and A. El Hallaoui, *Res. Chem. Intermed.*, **39**, 2417 (2013).
40. M. N. El-Haddad and K. M. Elattar, *Res. Chem. Intermed.*, **39**, 3135 (2013).
41. M. Gholami, I. Danaee, M. H. Maddahy, and M. RashyandAvei, *Ind. Eng. Chem. Res.*, **52**, 14875 (2013).
42. H. B. Ouici, O. Benali, Y. Harek, L. Larabi, B. Hammouti, and A. Guendouzi, *Res. Chem. Intermed.*, **39**, 3089 (2013).
43. S. Deng, X. Li, and X. Xie, *Corros. Sci.*, **80**, 276 (2014).
44. I. Ahamad, R. Prasad, and M. A. Quraishi, *Corros. Sci.*, **52**, 1472 (2010).
45. M. J. Bahrami, S. M. A. Hosseini, and P. Pilvar, *Corros. Sci.*, **52**, 2793 (2010).
46. L. Herrag, B. Hammouti, S. Elkadiri, A. Aouniti, C. Jama, H. Vezin, and F. Bentiss, *Corros. Sci.*, **52**, 3042 (2010).
47. A. S. El-Tabei and M. A. Hegazy, *J. Dispersion Sci. Technol.*, **35**, 1289 (2014).
48. A. S. Fouda, H. E. Megahed, T. Younis, and S. Abd El-Salam, *Prot. Met. Phys. Chem. Surf.*, **50**, 254 (2014).
49. H. Shokry, *J. Mol. Struct.*, **1060**, 80 (2014).
50. X. Li, S. Deng, H. Fu, and T. Li, *Electrochim. Acta*, **54**, 4089 (2009).
51. S. D. Deng, X. H. Li, and H. Fu, *Corros. Sci.*, **53**, 760 (2011).
52. S. E. Nataraja, T. V. Venkatesha, and H. C. Tandon, *Corros. Sci.*, **60**, 214 (2012).
53. M. Lagrenée, B. Mernari, M. Bouanis, M. Traisnel, and F. Bentiss, *Corros. Sci.*, **44**, 573 (2002).
54. S. K. Shukla and M. A. Quraishi, *Corros. Sci.*, **51**, 1007 (2009).
55. S. K. Shukla and M. A. Quraishi, *Corros. Sci.*, **52**, 314 (2010).
56. P. Lowmunkhong, D. Ungtharatak, and P. Sutthivaiyakit, *Corros. Sci.*, **52**, 30 (2010).
57. D. Özkır, K. Kayakırılmaz, E. Bayol, A. A. Gürten, and F. Kandemirli, *Corros. Sci.*, **56**, 143 (2012).
58. G. Moretti, F. Guidi, and F. Fabris, *Corros. Sci.*, **76**, 206 (2013).
59. H. Wu and Y. Li, *Electrochemical Kinetics*, Higher Education Press, Beijing (1998).